Temperature effect on emission spectra and fluorescence lifetime of the $^4I_{13/2}$ state of Er^{3+}-doped Gd_2SiO_5 crystal

Yuchong Ding (丁雨憧)[1,2], Guangjun Zhao (赵广军)[1*], Yosuke Nakai[3], and Taiju Tsuboi[3]

[1]*Key Laboratory of Materials for High Power Laser, Shanghai Institute of Optics and Fine Mechanics, Chinese Academy of Sciences, Shanghai 201800, China*

[2]*Graduate University of Chinese Academy of Sciences, Beijing 100039, China*

[3]*Faculty of Engineering, Kyoto Sangyo University, Kamigamo, Kita-ku, Kyoto 603-8555, Japan*

[*]*Corresponding author: zhaoguangjun@163.net*

Received February 16, 2011; accepted April 4, 2011; posted online June 21, 2011

By measuring the emission spectra and the fluorescence lifetime of the $^4I_{13/2}$ state of Er^{3+} ions in Gd_2SiO_5 crystal at different temperatures, the effects of temperature on the spectra and the lifetime of the $^4I_{13/2}$ state are investigated. When the temperature increases, the emission line width for the $^4I_{13/2} \rightarrow {}^4I_{15/2}$ transition is broadened, and the main emission lines at 1 596, 1 609, and 1 644 nm shifte toward shorter wavelengths. The measured lifetime of the $^4I_{13/2}$ state decreases from 13.2 to 8.4 ms with temperature increase from 13 to 300 K, which is mainly due to the temperature dependence of multiphonon relaxation between the $^4I_{13/2}$ and $^4I_{15/2}$ states and the changing population distribution among the Stark levels within the $^4I_{13/2}$ state. The experimental results imply that low temperature condition is better for the ~1.6-μm laser output.

OCIS codes: 160.3380, 300.6280, 160.5690

doi: 10.3788/COL201109.091602.

Recently, with the development of high-power InP laser diode and erbium fiber laser (EFL) in the 1.46−1.6-μm range[1,2], Er^{3+}-doped Gd_2SiO_5 crystal is considered to be an interesting material to obtain ~1.6-μm eyesafe laser based on the resonantly pumping sketch[3]. Compared with the well-known Er^{3+}:YAG crystal, Er^{3+}: Gd_2SiO_5 is anisotropic with monoclinic structure, belonging to the space group $P_{21/c}$[4], which means that it can be directly used to obtain polarized laser.

In the past several years, studies have been dedicated to the growth and spectroscopic characterization of Er^{3+}:Gd_2SiO_5, and some primary data are already available[5−7]. However, such data are not sufficient to predict laser performance, especially under different temperature conditions. Generally, increasing the temperature will result in thermal broadening and shift in the laser line, which have a significant meaning for the laser action since these effects are closely related to the light amplification gain, output frequency stability, and thermal tenability of the laser. The variation of fluorescent lifetime with the temperature is also significantly important for many Q-switched and other operations of Er^{3+}: Gd_2SiO_5 lasers. In this letter, the emission spectra of Er^{3+}:Gd_2SiO_5 at 13−300 K are measured, and the temperature dependence of the fluorescence lifetime for the $^4I_{13/2} \rightarrow {}^4I_{15/2}$ transition of Er^{3+} ions in this host has been studied.

Single crystals of Er^{3+}:Gd_2SiO_5 were grown from iridium crucible by Czochralski technique. The highly pure oxide powders Gd_2O_3 (99.999%), SiO_2 (99.999%), and Er_2O_3 (99.999%) were used as the starting materials, while the concentration of Er^{3+} ions in the melt was 0.3 at.-%. The seed was of <010> orientation and the whole growth atmosphere was high-purity nitrogen gas. The comparison of 2θ diffraction peak values and their corresponding relative intensity with the standard χ-ray diffraction (XRD) card of Gd_2SiO_5 indicates that the formation of the monoclinic structure of Gd_2SiO_5 was achieved in the Er^{3+}:Gd_2SiO_5 crystal that we have grown. The optical quality of the crystals was found to be good, as shown in Fig. 1. During the crystal growth of Er^{3+}:Gd_2SiO_5, the substitution of Gd^{3+} by Er^{3+} was accomplished easily because the dimensional, chemical, and physical properties of the two ions are quite similar. The sample used for spectroscopic measurements was optically polished, and the thickness of the sample was 1 mm.

The absorption spectrum of Er^{3+}:Gd_2SiO_5 was measured at 300 K by using a spectrophotometer (Lambda 900, Perkin-Elmer, USA). The emission spectra were measured with a spectrophotometer (Spex Fluorolog-3, Horiba, Japan) and were excited at 378 nm by a 450-W xenon lamp. The emission decay curves were obtained by pulse excitation with the 980-nm line of a diode laser. The emitting line of 1.528 μm for the $^4I_{13/2}$ manifold of Er^{3+}:Gd_2SiO_5 was detected through a 0.5-m monochromator with a photomultiplier. For the low temperature measurements, the Er^{3+}:Gd_2SiO_5 sample was cooled by a liquid-nitrogen cryogenic refrigerator, capable of controlling temperature from 13 to 300 K. For all the measurements, the spectral resolution was kept below 1 nm.

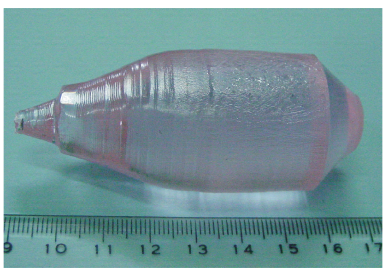

Fig. 1. Photo of as-grown Er^{3+}:Gd_2SiO_5 single crystal with size of Φ35×40 (mm).

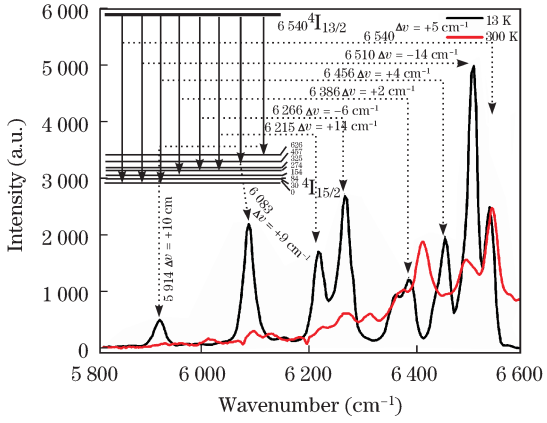

Fig. 2. Emission spectra of the $^4I_{13/2} \rightarrow ^4I_{15/2}$ transition at 13 and 300 K, and the Stark energy levels of the $^4I_{15/2}$ state, as well as the line shift value ($\Delta\nu$) aside the dot line.

The emission spectrum at 13 K for the $^4I_{13/2} \rightarrow ^4I_{15/2}$ transition is shown in Fig. 2 (black curve). As most of Er^{3+} ions are frozen at the lowest Stark level of the $^4I_{13/2}$ state, transitions from this level to all the Stark levels of the $^4I_{15/2}$ state give off eight main emission lines (i.e., 5 914, 6 083, 6 215, 6 266, 6 386, 6 456, 6 510, and 6 540 cm^{-1}), but the remaining weak emission lines (such as 6 361 cm^{-1}) originate from thermally populated excited levels within the $^4I_{13/2}$ state. The zero line is 6 540 cm^{-1}, and the Stark splitting of the $^4I_{15/2}$ state are calculated to be 0, 30, 80, 146, 270, 320, 458, and 628 cm^{-1}, which are in agreement with the data reported in Ref. [7]. Figure 3 shows the temperature evolution of the $^4I_{13/2} \rightarrow ^4I_{15/2}$ emission spectra in the temperature range of 13−300 K. The greatest influence of temperature is on the spectra shape and emission intensities. At low temperatures, the individual lines are well separated from each other; with increasing temperature, each individual line becomes broad and gradually overlaps with the neighboring lines arising from the higher Stark levels. When the temperature was increased from 13 to 300 K, the effects of thermal populations on the Stark levels within the $^4I_{13/2}$ state not only extended the short wavelength edge of the emission spectra from 1.520 to 1.440 μm, but also smoothened down the emission intensities of the main lines. For the relatively intense emission lines at 1.596, 1.609, and 1.644 μm, when the temperature increased from 13 to 300 K, their emission intensities decreased by 4, 4.5, and 6 times, respectively. Since their terminating levels are separated by 457, 325, and 274 cm^{-1} from the lowest Stark level of the $^4I_{15/2}$ state (the inset of Fig. 2), thermodynamic calculation using Boltzmann distribution demonstrates that decreasing temperature will reduce the thermal population at these levels, resulting in weak reabsorption at these lines. On the contrary, the lines shorter than 1.560 μm encountered intense reabsorption, as presented in Fig. 4, by comparing the absorption and emission spectra at different temperatures. In this point of view, Er^{3+}:Gd_2SiO_5 may have potential to realize laser oscillation at the 1.596-, 1.609-, and 1.644-μm lines, especially on the conditions of low temperatures.

On the other hand, the line positions are also temperature dependent due to the stationary effect of the ion–phonon interaction. Electron–phonon interactions perturb various electronic states, changing their wave functions and energies. The greater the distance from neighboring atoms is, the lower will be the potential of the crystal field of an impurity ion and the smaller the stark splitting of its multiplets as the temperature of the crystal increases[8]. For Er^{3+}:Gd_2SiO_5 lattice, thermal expansion can reduce the crystal field of Er^{3+} ions, resulting in weakened Stark splitting as temperature increases. This effect not only acts on the $^4I_{13/2}$ state but also on the $^4I_{15/2}$ state; thus, their Stark levels will shift toward lower or higher energies as the temperature increases. From Fig. 3, the emission lines at 1.529, 1.549, 1.566, 1.609, 1.644, and 1.690 μm shift to shorter wavelengths and the lines at 1.536 and 1.596 μm shift to longer wavelengths. Aside the dot line of Fig. 2 labels the line shift value ($\Delta\nu$) for each emission line; the largest red-shift occurred at 1.536 μm with 14 cm^{-1} and the line at 1.609 μm encountered the largest blue-shift with 14 cm^{-1} as the temperature increased from 13 to 300 K.

The emission decays of the $^4I_{13/2} \rightarrow ^4I_{15/2}$ transition measured at different temperatures are depicted in Fig. 5. All the decay curves have nearly single-exponential

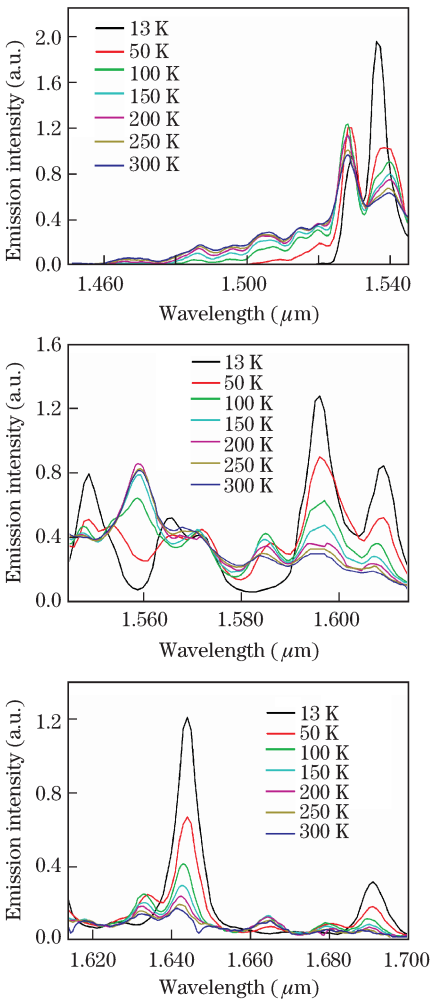

Fig. 3. Temperature evolution of the emission spectra from 13 to 300 K for the $^4I_{13/2} \rightarrow ^4I_{15/2}$ transition of Er^{3+}: Gd_2SiO_5.

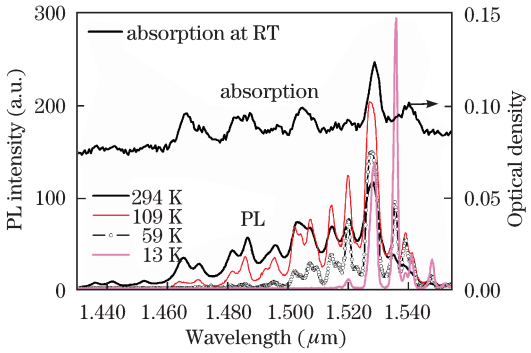

Fig. 4. High-resolution photoluminescence (PL) spectra of the Er^{3+}-doped Gd_2SiO_5 crystal excited at 378 nm at various temperatures, compared with the absorption spectrum at room temperature (RT); the PL measurement is done at spectral resolution of 0.6 nm.

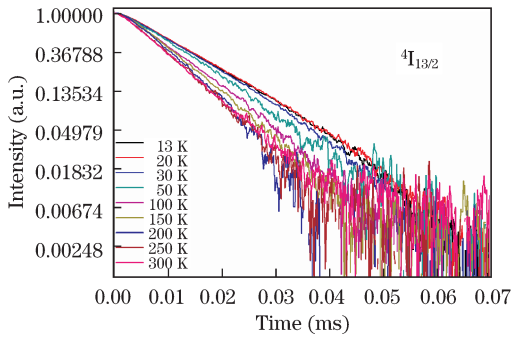

Fig. 5. Fluorescence decays relate to the $^4I_{13/2} \rightarrow {}^4I_{15/2}$ transition.

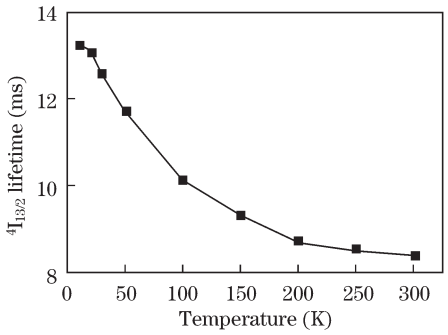

Fig. 6. Measured lifetime for the $^4I_{13/2}$ manifold at different temperatures.

behavior, which indicates that the effects of concentration quenching and upconverison can be neglected in low Er^{3+}-doped Gd_2SiO_5. Figure 6 shows the temperature dependence of the fluorescence lifetime of the $^4I_{13/2}$ state in the range of 13−300 K. The values of fluorescence lifetime monotonously decreased from 13.2 to 8.4 ms when the temperature increased from 13 to 300 K. This result arose from several sources: the multiphonon transition between the $^4I_{13/2}$ and $^4I_{15/2}$ states is temperature dependent[9], which directly affects the fluorescence lifetime of the $^4I_{13/2}$ state. In this multiphonon process, the highest energy phonons are usually considered to make the dominant contribution to this process since they conserve energy in the lowest-order process. However, Er^{3+}:Gd_2SiO_5 crystal has many high-density phonons such as 344, 547, and 883 cm^{-1} beside the highest-energy phonon at 998 cm^{-1}, as shown in Fig. 7 (the dominant Raman shifts around 943, 547, 418, 344, and 171 cm^{-1} can be attributed to the symmetric stretching vibration, anti-symmetric stretching vibration, and bending vibration of $(SiO_4)^{4-}$ tetrahedron[10]; the contributions of the lower-energy phonons process or combinations of phonons process cannot be neglected. Furthermore, in Er^{3+}:Gd_2SiO_5 lattice, Er^{3+} ions substitute for Gd^{3+} in two sites, which are coordinated by seven and nine oxygen ions, respectively. The coupling of vibrations to the Er^{3+} ions at the two sites is not identical. Thus, it is impossible to depict the multiphonon process quantitatively for the $^4I_{13/2} \rightarrow {}^4I_{15/2}$ transition, and its temperature dependence is roughly consistent with the overall trend of the experimental data. In addition, the crystal field effect and the changing population distribution among Stark levels having different radiative and non-radiative decay probabilities are also responsible for the lifetime drop when the temperature increases[11]. The temperature dependence of the lifetime of the $^4I_{13/2}$ state implies that the fluorescence quantum efficiency η ($\eta = \tau_f/\tau_{sp}$, where τ_f and τ_{sp} denote the fluorescence lifetime and the radiative lifetime, respectively) of the $^4I_{13/2} \rightarrow {}^4I_{15/2}$ transition at 13 K is about 1.6 times larger than that at 300 K, which means that the low temperature condition is better for the ∼1.6-μm laser operation.

In conclusion, Er^{3+}:Gd_2SiO_5 single crystal with good optical quality is successfully grown by the Czochralski method. The temperature effect on the emission spectra and the fluorescence lifetime of the $^4I_{13/2}$ state are investigated. When the temperature is increased from 13 to 300 K, the main emission lines are broadened. For the potential laser lines of 1.596, 1.609, and 1.644 μm, the emission intensities decrease by 4, 4.5, and 6 times, respectively. The emission line positions are also temperature dependent. The largest red-shift occurred at 1.536 μm with 14 cm^{-1}, and the line at 1.609 μm encountered the largest blue-shift with 14 cm^{-1}. The fluorescence lifetime of the $^4I_{13/2}$ state for Er^{3+}:Gd_2SiO_5 crystal clearly decreased with the increase in temperature. It was about 13.2 ms at 13 K and decreased to

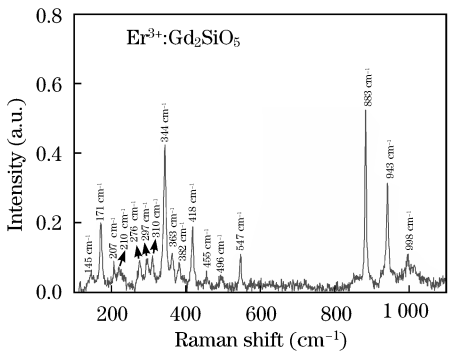

Fig. 7. Raman spectrum of Er^{3+}: Gd_2SiO_5 crystal (it is recorded using a spectrometer (INVIA, Renishow, England) equipped with a monochromator, a filter system, and charge-coupled device detector; unpolarized 785-nm laser from a laser diode is chosen as the excitation light).

8.4 ms at 300 K. This is mainly ascribed to the temperature dependence of multiphonon relaxation between the $^4I_{13/2}$ and $^4I_{15/2}$ states and the changing population distribution among the Stark levels within the $^4I_{13/2}$ state. All the experimental data imply that low temperature is beneficial to realize laser oscillation at the potential laser lines of 1.596, 1.609, and 1.644 μm.

This work was supported by the National Natural Science Foundation of China under Grant No. 90922029.

References

1. X. Mao, F. Yan, Y. Fu, L. Wang, J. Peng, L. Liu, and S. Jian, Chin. Opt. Lett. **7,** 993 (2009).
2. B. Lei and Y. Feng, Chin. Opt. Lett. **7,** 1018 (2009).
3. S. D. Setzler, M. P. Francis, Y. E. Young, J. R. Konves, and E. P. Chicklis, IEEE J. Selected Topics Quant. Electron. **11,** 645 (2005).
4. J. Felche, *Structure and Bonding* (Springer, Berlin, 1973).
5. Y. Zong, G. Zhao, C. Yan, X. Xu, L. Su, and J. Xu, J. Crystal Growth **294,** 416 (2006).
6. X. Xu, G. Zhao, F. Wu, W. Xu, Y. Zong, X. Wang, Z. Zhao, G. Zhou, and J. Xu, J. Crystal Growth **310,** 156 (2008).
7. A. S. S. de Camargo, M. R. Davolos, and L. A. Nunes, J. Phys. Condens. Matt. **14,** 3353 (2002).
8. M. Eichhorn, S. T. Fredrich-Thornton, E. Heumann, and G. Huber, Appl. Phys. B **91,** 249 (2008).
9. L. A. Riseberg and H. W. Moos, Phys. Rev. **174,** 429 (1968).
10. P. Dawson, M. M. Hargreav, and G. R. Wilkinso, J. Phys. Part C . **4,** 240 (1971).
11. R. D. Shannon, Acta Crystallog. A **32,** 751 (1976).